Rocznik Ochrona Środowiska

Volume 28 Year 2026 ISSN 2720-7501 pp. 181-195

https://doi.org/10.54740/ros.2026.014 open access

Received: January 2026 Accepted: March 2026 Published: April 2026

Modelling Rainfall Prediction with Quantum Circuits on the SPINQ Gemini Lab Pro Platform

Mariselvam A.K.[1], S. Mohamed Nizar[2], S. Sasikumar[3], Vieeralingaam G.[4]*

[1]*Rajalakshmi Institute of Technology, The Grover Centre of Quantum Technology, Chennai, India*
https://orcid.org/0000-0003-3612-4657

[2]*Rajalakshmi Institute of Technology, The Grover Centre of Quantum Technology, Chennai, India*
https://orcid.org/0000-0003-4254-7744

[3]*Rajalakshmi Institute of Technology, The Grover Centre of Quantum Technology, Chennai, India*
https://orcid.org/0000-0001-9732-3268

[4]*Rajalakshmi Institute of Technology, The Grover Centre of Quantum Technology, Chennai, India*
https://orcid.org/0000-0001-6276-4100

**corresponding author's e-mail: mariselvamak@gmail.com*

Abstract: Here, we propose a quantum circuit-based model to predict rainfall using nonlinear meteorological variables, grounded in quantum computational principles. The qubits are encoded with temperature, pressure, and humidity using the $R_y(\theta)$ gate, and the CNOT gate is used for entangling the qubits to gain inter-variable correlations. $R_z(\theta)$ and $R_x(\theta)$ gates are also used to enhance the circuit's ability to represent complex weather patterns. The model is validated using meteorological data consisting of Temperature, Pressure, and Humidity measurements collected between August 1 and August 31, 2025. The model achieved a theoretical fidelity of 87.99% in predicting rainfall conditions. Using the SPINQ Gemini quantum platform, the model is implemented experimentally and achieved a quantum state purity of 100% to score a practical fidelity of 82.62%, indicating a high probability of rainfall with a density matrix of ($|0\rangle$ = 0.04, $|1\rangle$ = 0.96). The consistency between theoretical and practical outcomes is shown by rainfall accuracy of 87.99% and no-rainfall accuracy of 12.01%. These results show the potential of data-driven prediction in the future and of rainfall prediction using quantum circuits.

Keywords: Quantum circuit, temperature, pressure, and humidity, Entanglement, CNOT gates

1. Introduction

Accurate weather prediction is beneficial for agriculture, disaster management, transportation, and urban planning. Traditional numerical weather prediction (NWP) is highly compatible at large scales by solving complex physical equations that simulate atmospheric dynamics (Palmer et al., 2005). But NWP models give poor predictions of the weather for short-term or local forecasts due to limitations in grid resolution and the computational complexity of the equations (Bauer et al., 2015). To combat this, machine learning (ML) is used on the complex equations that can be solved with nonlinear relationships between atmospheric variables, datasets to complex model (Rasp & Lerch, 2018). Meteorological parameters such as dew point, wind gusts, cloud cover, air pressure, humidity, air temperature, wind speed, wind direction, and rainfall can be used in an Artificial Neural Network (ANN) model to improve prediction accuracy (Pratomo et al., 2022). When it comes to high-resolution, real-time predictions, classical ML models lack the ability to scale or compute efficiently as datasets grow in size.

Quantum computing exploits quantum properties such as superposition, entanglement, and interference to compute certain solutions exponentially faster than the traditional classical method (Nielsen & Chuang, 2010). Data processing can be sped up exponentially, and the expressivity of the ML model increased by integrating quantum with classical ML models, a field called Quantum Machine Learning (QML) (Biamonte et al., 2017). Variational Quantum Circuits (VQC) is a practical approach that optimises the training for predictive tasks by tuning quantum gates within a hybrid quantum-classical framework (Farhi & Neven, 2018; Schuld et al., 2020). The groundwork for the QML is laid by the theoretical framework for quantum-enhanced supervised learning studied by V. Havlíček et al. (2019) and M. Benedetti et al. (2019), which uses quantum feature spaces and parameterised quantum circuits.

In a region, rainfall data collected over a long term show temporal and spatial variability. Jayawardene et al. observed large changes in the precipitation over a century in Sri Lanka in 2005 (Jayawardene, 2005). Similarly, Shahid observed an increase in the occurrence of extreme rainfall in Bangladesh in 2011 (Shahid., 2011). In China, Su et al. observed increases in temperature and extreme rainfall in the Yangtze River Basin in 2006 (Su et al., 2006). Regions such as Amman, Jordan, show shifts in rainfall patterns during the mid-20th century, indicating harsh climatic variability in semi-arid climates (Smadi & Zghoul, 2006). Wilson

et al. (2013) showed that certain large-scale atmospheric patterns can influence regional rainfall in parts of southern Queensland. In 2014, Olatayo and Taiwo developed statistical and computational models to apply time-series analysis to predict rainfall (Olatayo & Taiwo, 2014). In Malaysia, Pour et al. used genetic programming to downscale extreme rainfall events (Pour et al., 2014).

Despite advances in modelling techniques, the nonlinear relations among atmospheric variables lead to uncertainties in predicting weather and climate. Slingo and Palmer stated the fundamental limits to the accuracy of predictions in 2011, as noted in the theoretical models proposed by Rotunno and Snyder in 2008 (Slingo & Palmer, 2011; Rotunno & Snyder, 2008). Precipitation patterns are continuously modified by climate change, so it is essential to understand the regional impacts. The University Corporation for Atmospheric Research (UCAR) states that such changes should be studied to plan with disaster management and adaptation strategies by the UCAR Center for Science Education.

In this study, using the SPINQ Gemini Lab Pro platform, we proposed a quantum-circuit-based hybrid model to predict rainfall. The $R_y(\theta)$ gates are used to encode temperature, pressure, and humidity, which are encoded as quantum rotations. CNOT gates are used to model the correlation between the variables. $R_z(\phi)$ and $R_x(\phi)$ gates are used to train the circuits, where the parameters $\phi 0$ and $\phi 5$ are optimized by a loss function that compares the real data to the predicted data. Measurement is performed over multiple shots to estimate the probability of rain.

2. Materials and Methods

The Hybrid Quantum-Classical framework has been applied to implement the proposed Qurain Model using the following methods: Classical computation for data preprocessing and normalization, and for parameter optimization. Quantum computation is being used to encode features and learn them from the data. The design, simulation, and hybrid execution of quantum circuits were performed on Qiniverse, a cloud-computing platform for quantum computing that supports parameterized quantum circuits and variational algorithms. To verify feasibility for execution on physical hardware, selected circuits with low qubit counts were run on SpinQ quantum systems that employ Nuclear Magnetic Resonance (NMR)-based quantum preprocessing at a desktop scale.

Using typical normalization techniques and interpolation techniques, the preprocessing of historical rainfall and geospatial datasets was completed as required for use with quantum computers. Data dimensionality reduction was completed, based on existing quantum hardware limitations. Classical features were converted into quantum states via angle-based coding. Construction, execution, and evaluation of constructed parameterized quantum circuits were performed utilizing single rotation rotational gates and entangling gates contained within the circuits using the Qiniverse quantum computer simulator before running shallow equivalents on the SpinQ quantum computer hardware (Figure 1). Classical Gradient-free optimization techniques were employed using the actual measurement results from the execution and modelling phase to find optimal parameter values of the parameterized quantum circuit. The proposed Qrain methodology is reproducible across different quantum platforms and simulation software. The generated circuit is constructed using standard gate-level operations. Also, these operations are performed using commonly available frameworks such as IBM's Qiskit. Since normalization of the input features is achieved by mapping angles onto the parameters of the normalized radial wind and precipitation, the physical structure of the circuit can be used on all quantum platforms, except for minor differences in performance due to hardware noise characteristics.

Qrain is likely to expand its ability to process sensor readings (temperature, pressure, and humidity) from IoT-linked meteorological sensors and automated weather stations into real-time data using traditional preprocessing methods. These methods will allow continuous measurement of sensor data, supplying a constant stream of temperature, pressure, and humidity data to a traditional preprocessing unit for continual collection. Additionally, after these third-party sensors are normalized to remove as much measurement difference as possible, Qrain will dynamically map all three sensor parameters into the quantum rotation parameters ($R_y(\theta)$) of the Qrain model. Because the Qrain model uses parameterized quantum gates rather than fixed datasets, it can process sensor stream inputs in real time. The Qrain model's hybrid classical/quantum framework is designed for this application; traditional sensors collect and preprocess environmental sensor data, while the quantum processor executes Qrain-encoded circuits. Therefore, using the Qrain methodology, it may soon be feasible to establish real-time environmental monitoring systems as soon as quantum hardware becomes widely available, with little latency (delay) or processing time associated with the execution of rainfall predictions.

Fig. 1. 3-Qubit NMR quantum computer

3. Results and Discussions

By exploiting quantum entanglement, quantum computing can solve nonlinear relations and complex data-driven tasks such as weather prediction. Here, we present a quantum circuit-based model that predicts rainfall probability from live measurements of weather parameters (temperature, pressure, and humidity). Using the SPINQ Gemini Lab Pro platform, the presented model is implemented and verified to process weather data by efficiently converting values to quantum states.

The quantum circuit consists of three qubits; temperature, pressure, and humidity are encoded into qubits q_0, q_1 and q_2 respectively. The final output from the measurement is considered a rain or no-rain case. The data are encoded using $R_y(\theta)$ gates to rotate the qubits. Where the θ is calculated using Eqn. (1).

$$\theta = \pi \frac{x - x_{min}}{x_{max} - x_{min}} \tag{1}$$

This ensures that all input parameters are normalized and bounded between 0 and π radians, allowing them to be properly represented as quantum rotations. Entanglement between qubits is introduced using CNOT gates to capture interactions among temperature, pressure, and humidity. Following this, variational layers composed of parameterized $R_z(\phi)$ and $R_x(\phi)$ gates are applied, where $\phi 0$ to $\phi 5$ are trainable parameters. These ϕ parameters serve as tuneable knobs that the learning algorithm adjusts to model complex relationships in the data, such as how high humidity combined with high temperature increases the likelihood of rain, while high pressure reduces it. Initially set randomly, the ϕ values are optimized through a hybrid quantum-classical approach, minimizing a loss function defined by the squared error between predicted and actual rainfall data.

Measurement is performed on the third qubit (q_2) after multiple runs (shots) of the quantum circuit. The probabilistic nature of quantum computing necessitates running the circuit many times, for example, 1024 shots, to collect a distribution of outcomes. The final rain prediction probability is calculated by summing the probabilities of all measured states where the output qubit is in state $|1\rangle$, indicating rain. This process is fully integrated into the SPINQ Gemini Lab Pro software, which provides histograms of outcome frequencies, enabling direct extraction of rain probability without manual calculations.

The classical part of the system handles data storage, loss computation, parameter optimisation, and normalisation. The sensor data are fetched from the dataset, which stores the past weather data on a classical computer and converted to rotational angles for the quantum processor. After the quantum circuit runs and outputs probabilistic measurements, the loss function is used to compare the predicted value to the historical value by the classical optimiser. The optimiser modifies the ϕ parameters using the loss function until convergence occurs. Accurate rainfall is achieved with the optimal parameter set, converged by the hybrid training loop.

After the hybrid training loop, the quantum circuit model can predict the rainfall probability in steps by reading the temperature, pressure, and humidity data, converting them into angles, running the circuit, and measuring the output. The classical part comes into play by managing the data flow, comparing to find the loss, and updating the parameter. The computational hardness faced by classical models is easily overcome by a quantum circuit. This shows the potential of quantum machine learning in real-world applications. The circuit diagram is shown in Fig. 2.

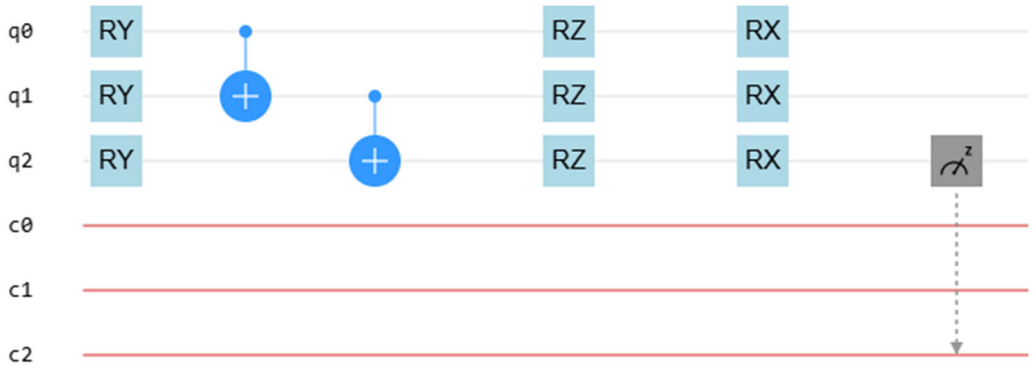

Fig. 2. Circuit diagram for Rainfall Prediction

Assuming q_0 represents Temperature, q_1 represents Pressure, and q_2 represents Humidity. Initially, each qubit starts in the state $|0\rangle$, meaning that q_0, q_1, and q_2 are all in their ground states corresponding to these respective variables.

Firstly, the R_y rotations are applied to each qubit, which is considered to encode the data via superposition. The q_0 (Temperature) qubit is given a 144° rotation, q_1 (Pressure) qubit is given a 3.6° rotation, q_2 (Humidity) qubit is given a 135° rotation, which leaves all 3 qubits in a superposition state. Next, using the CNOT gates, entanglement is created by entangling q_0 with q_1, followed by entangling q_1 with q_2 establishing the quantum correlations among temperature, pressure, and humidity. Finally, R_z and R_x gates are to apply further phase shifts and rotations. For q_0, R_z is 90° and R_x is 90°, for q_1, R_z is 90° and R_x is 85°, and for q_2, R_z is 90° and R_x is 180°. The R_z gates are used to shift the phase of the qubits and the R_x gates are used to change the state of the qubits.

The R_z and R_x gates play an important role by shifting the phase and amplitude of the qubits, thereby influencing their interaction. To generate these, directly control the quantum states to affect the final outcome and produce a good prediction. The change in interference patterns modifies the probability amplitude due to the shift in qubit amplitudes and relative phase difference caused by the R_z and R_x gates. The model's accuracy can be increased when the phase of the entanglement qubits is changed, which affects the quality of the entanglement and influences the final output. To change these angles effectively, you can manually tune them by testing fixed values like 45°, 90°, 135°, or 180° and observing their effects. Alternatively, you can use parameter optimization methods in variational quantum circuits, where R_x and R_y angles are treated as parameters optimized via classical algorithms, such as gradient descent or Nelder-Mead, to find the best-performing configuration. With quantum superposition, an individual can have multiple probabilistic states represented at the same time through quantum-mechanical means, thus increasing representational capacity, while entanglement provides a way to capture correlations that are not linear amongst meteorological variables. When combined, these two quantum phenomena enhance a model's expressive capability, resulting in improved accuracy in predictions. Tuning the rainfall predictor for different degrees is shown in Fig. 3.

Table 1 shows the predicted rainfall and no-rain percentages for various combinations of rotation angles R_x and R_z in the quantum circuit model. The results indicate a strong dependence of rainfall prediction on the choice of rotation angles, highlighting the variational quantum circuit's sensitivity to parameter tuning. Across all combinations, the highest rainfall prediction of 87.99% occurs at R_z = 45° and R_x = 135°, accompanied by a low no-rain probability of 12.01%, demonstrating the optimal configuration for the given dataset. Other high rainfall predictions (>86%) are observed at R_z = 90°/135° with R_x = 135°, showing consistent performance around these parameter ranges.

Conversely, lower rainfall predictions (<30%) occur for smaller R_x angles (45°) combined with lower R_z values (45–90°), suggesting that insufficient rotation limits the circuit's ability to encode complex correlations among meteorological variables. No-rain probabilities inversely mirror these trends, with maximum no-rain likelihoods (>70%) corresponding to low predicted rainfall percentages.

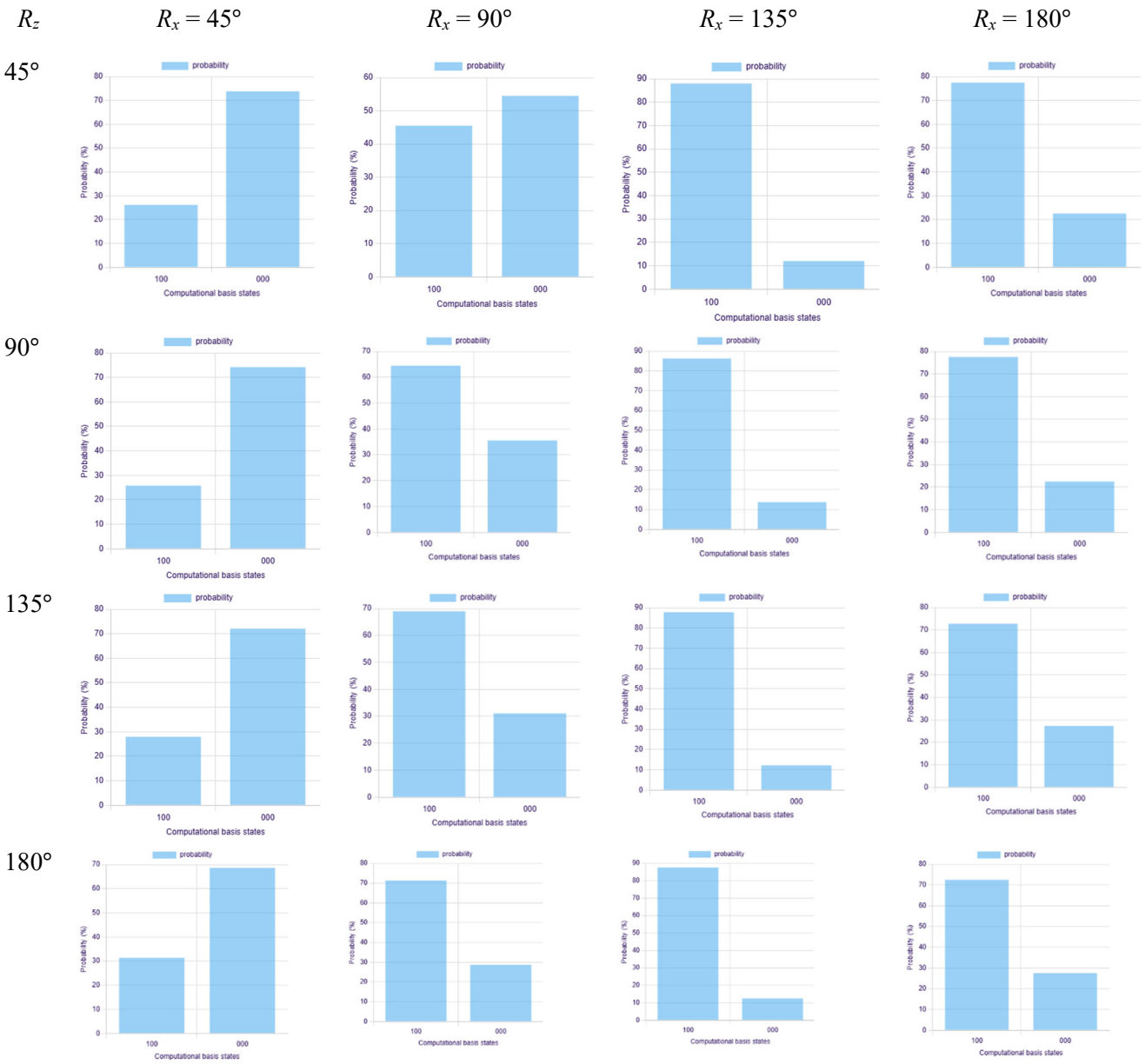

Fig. 3. Tuning the Qurain by testing fixed values like 45°, 90°, 135°, or 180°

Table 1. Predicted rainfall percentages for different combinations of rotation angles

R_z(°)	R_x(°)	Rain (%)	No Rain (%)
45	45	26.17	73.83
45	90	45.51	54.49
45	135	87.99	12.01
45	180	77.44	22.56
90	45	25.78	74.22
90	90	64.45	35.55
90	135	86.23	13.77
90	180	77.55	22.46
135	45	27.93	72.07
135	90	68.95	31.05
135	135	87.79	12.21
135	180	72.75	27.25
180	45	31.35	68.65
180	90	71.29	28.71
180	135	87.85	12.5
180	180	72.46	27.54

From Table 2, it can be inferred that the optimal output in the Qurain quantum circuit is obtained when R_x = 135° and R_z = 45°, and more generally, the setting R_x = 135° consistently yields the best results for different values of R_z; this behaviour can be explained by examining the geometric action of rotations on the Bloch sphere, where the R_x gate rotates the qubit around the x-axis and, at 135°, moves the initial |0⟩ state from the north pole to a position close to the equatorial plane but slightly biased toward |1⟩, thereby creating a balanced superposition in which both |0⟩ and |1⟩ components have significant amplitudes and are highly sensitive to subsequent phase shifts; when the R_z gate is applied after this rotation, which meaningfully alters the relative phase of the superposition, producing constructive interference patterns that directly influence measurement outcomes, whereas smaller R_x values (such as 0° or 45°) keep the state closer to |0⟩ where R_z has negligible effect, and R_x = 180° pushes the state near |1⟩ where Rz again loses impact, making R_x = 135° the "sweet spot" that provides the right balance between amplitude mixing and phase sensitivity**,** and thus explains why this angle consistently produces superior results across different R_z values.

Table 2. Rain/No-Rain Percentages for Different R_x and R_z Rotation Angles

R_z (Deg)	R_x = 45°	R_x = 90°	R_x = 135°	R_x = 180°
45	26.17/73.83	45.51/54.49	87.99/12.01	77.44/22.56
90	25.78/74.22	64.45/35.55	86.23/13.77	77.55/22.46
135	27.93/72.07	68.95/31.05	87.79/12.21	72.75/27.25
180	31.35/68.65	71.29/28.71	87.85/12.50	72.46/27.54

*Values are in Percentage.

It is observed that the prediction improves beyond 45°. However, as the angle decreases from 45° to 30°, the probability of rain increases. This indicates that R_z = 30° provides a comparatively better result. The result for R_z = 30° and R_x = 135° is shown below in Figure 4. This result is not used in Qurain because, in the Quantum Qurain setup, the rotation angle R_x directly determines the measurement probabilities, which follow a sinusoidal law of $\sin^2(\theta/2)$ and $\cos^2(\theta/2)$. At R_x = 45°, the state achieves constructive alignment, producing a stable bias in favour of one outcome and thereby maximizing prediction accuracy. Although at R_x = 35° the result may appear good, this region lies on a steeper slope of the probability curve, making it highly sensitive to noise and fluctuations, which reduces reliability. As R_x increases beyond 45°, the Bloch vector moves away from the measurement axis, causing the constructive interference to diminish and the outcome probabilities to spread more evenly between states. This shows that while angles slightly below 45° may look acceptable, exceeding 45° inevitably degrades prediction accuracy, making 45° the effective upper limit for stable results in this circuit.

The probability of measurement, expressed as a percentage, is shown on the vertical axis of Figure 4, which is a non-dimensional quantity. Probability is a number between 0 and 1, so it has no dimension or unit associated with it; however, it has been displayed as a % for your understanding. The horizontal axis represents the basis states (|100⟩ and |000⟩) that can be obtained through any computation process, which are both discrete quantum states and also have no units.

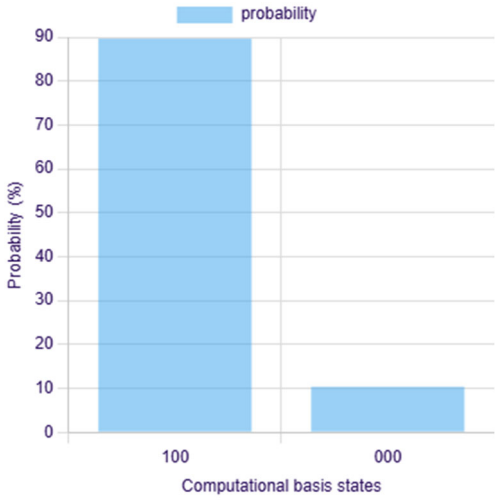

Fig. 4. Result for R_z = 30° and R_x = 135° (Rain = 89.55%; No Rain = 10.45%)

A probabilistic analysis of rainfall and no-rain events from 1 August 2025 to 31 August 2025 (Courtesy: TNPCB) for the Royapuram, Tamil Nadu, location was carried out using the proposed quantum circuit–based model. The histogram of the results highlights the system's predictive capability. The model predicted a 90.43% chance of rain and a 9.47% chance of no rain on 20th August 2025. It also predicted a 96.68% chance of rain and a 3.32% chance of no rain. These results show that accurate predictions of rainfall probability can be obtained from the quantum rainfall predictor. Quantum mechanics, such as entanglement and variational optimisation, shows great potential for efficiently encoding data into quantum states and can be scaled up to develop accurate quantum weather prediction models.

Table 3. Percentage of Rain and No rain for august 2025

S.No	Date	Temperature (°)	Pressure (°)	Humidity (°)	Rain (%)	No Rain (%)
1	01-08-2025	127	47	129	62.30	37.70
2	02-08-2025	128	48	134	63.48	36.52
3	03-08-2025	128	47	135	83.98	16.02
4	04-08-2025	127	48	134	51.07	48.93
5	05-08-2025	126	48	139	73.34	26.66
6	06-08-2025	126	47	135	3.32	96.68
7	07-08-2025	127	47	135	39.36	60.64
8	08-08-2025	127	47	136	42.38	57.62
9	09-08-2025	125	47	138	88.38	11.62
10	10-08-2025	126	48	134	40.53	59.47
11	11-08-2025	126	49	135	64.45	35.55
12	12-08-2025	125	50	136	69.73	30.27
13	13-08-2025	129	49	139	64.75	35.25
14	14-08-2025	123	50	135	8.79	91.21
15	15-08-2025	124	49	129	45.02	54.98
16	16-08-2025	125	49	136	54.69	45.31
17	17-08-2025	123	50	144	85.64	14.36
18	18-08-2025	122	50	137	60.55	39.45
19	19-08-2025	122	51	122	25.00	75.00
20	20-08-2025	126	50	122	90.53	9.47
21	21-08-2025	127	49	129	54.00	46.00
22	22-08-2025	126	50	143	46.29	53.71
23	23-08-2025	122	49	149	44.63	55.37
24	24-08-2025	125	51	134	67.97	32.03
25	25-08-2025	123	51	132	81.74	18.26
26	26-08-2025	124	49	134	53.61	46.39
27	27-08-2025	124	49	133	56.93	43.07
28	28-08-2025	125	49	130	50.49	49.51
29	29-08-2025	127	48	131	50.49	49.51
30	30-08-2025	126	48	130	36.04	63.96
31	31-08-2025	126	47	159	39.26	60.74

Note – The degree (°) in the table denotes angular encoding for quantum processing, not the original physical units. The meteorological data were mapped into angles before circuit implementation.

Table 3 and Figure 5 present rainfall prediction results for the period August 1–31, 2025, demonstrating the effectiveness of the proposed quantum-based approach in capturing daily precipitation patterns using temperature, pressure, and humidity as input variables. The predicted rainfall probabilities vary significantly across the month, ranging from 3.32% on August 6 to 90.53% on August 20, indicating that the model is sensitive to changes in meteorological conditions. Correspondingly, the no-rain probabilities inversely reflect

these variations, with higher values during low rainfall likelihoods (e.g., 96.68% on August 6) and lower values during high rainfall events (e.g., 9.47% on August 20).

The model successfully identifies extreme rainfall events, such as on August 3, 9, 17, 20, and 25, where rainfall probabilities exceed 80%, while also accurately capturing dry periods, such as on August 6 and 14, where rain probabilities fall below 10%. Moderate rainfall events (40–70%) are well-represented across transitional days, highlighting the model's capacity to handle nonlinear relationships among temperature, pressure, and humidity. Overall, the analysis of one-month data indicates that the proposed method achieves high predictive reliability and can differentiate between rain and no-rain days. The results further validate the potential of quantum-inspired or hybrid quantum-classical models for short-term rainfall forecasting based on meteorological data, providing actionable insights for planning in sectors sensitive to precipitation patterns. A bar chart representation of the rainfall prediction for August 2025 is shown below.

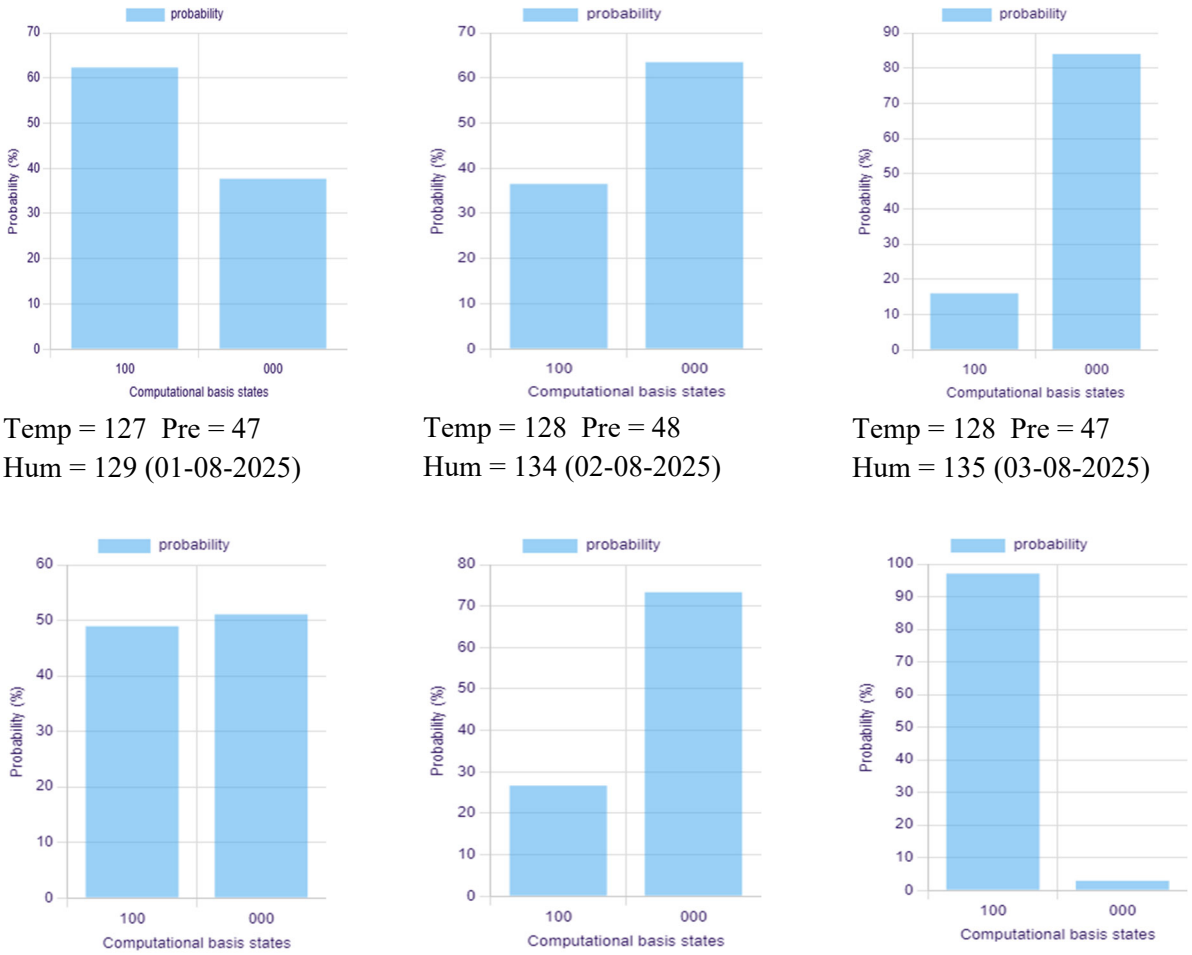

Temp = 127 Pre = 47
Hum = 129 (01-08-2025)

Temp = 128 Pre = 48
Hum = 134 (02-08-2025)

Temp = 128 Pre = 47
Hum = 135 (03-08-2025)

Temp = 127 Pre = 48
Hum = 134 (04-08-2025)

Temp = 126 Pre = 48
Hum = 139 (05-08-2025)

Temp = 126 Pre = 47
Hum = 135 (06-08-2025)

Fig. 5. Bar Chart Output Showing Rainfall Prediction for August 2025

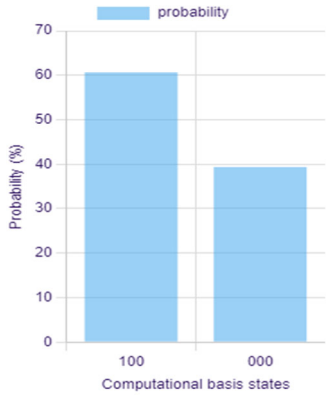

Temp = 127 Pre = 47
Hum = 135 (07-08-2025)

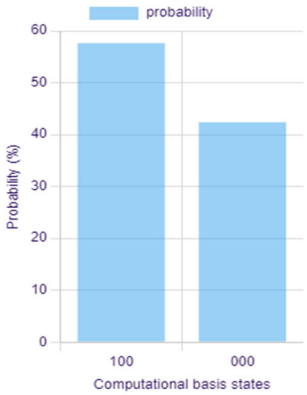

Temp = 127 Pre = 47
Hum = 136 (08-08-2025)

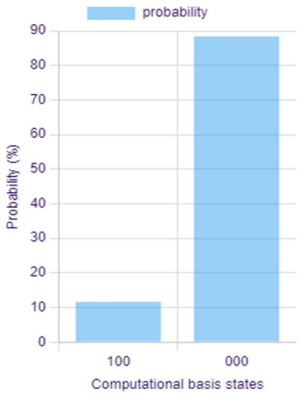

Temp = 125 Pre = 47
Hum = 138 (09-08-2025)

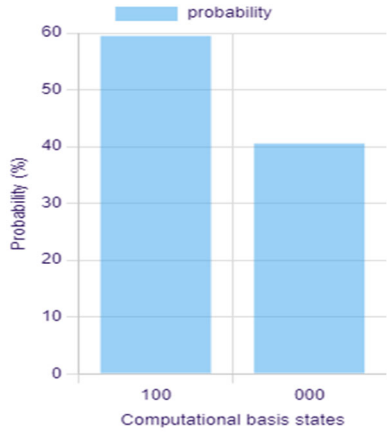

Temp = 126 Pre = 48
Hum = 134 (10-08-2025)

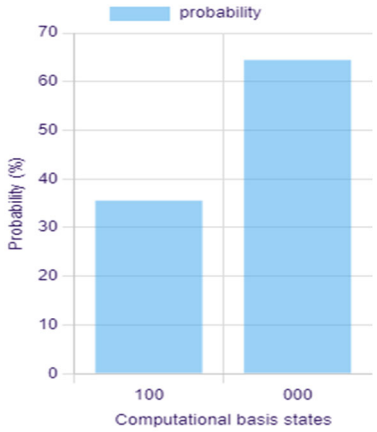

Temp = 126 Pre = 49
Hum = 135 (11-08-2025)

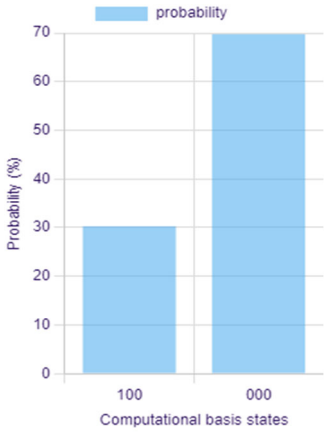

Temp = 125 Pre = 50
Hum = 136 (12-08-2025)

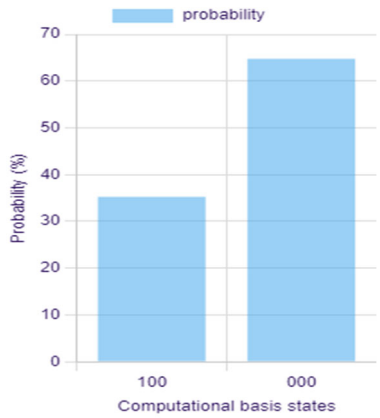

Temp = 129 Pre = 49
Hum = 139 (13-08-2025)

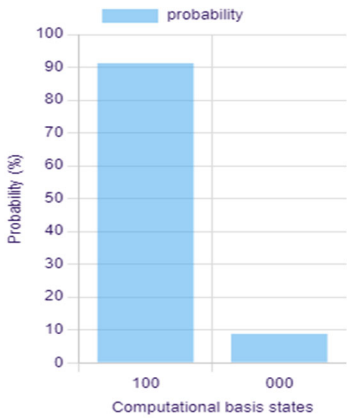

Temp = 123 Pre = 50
Hum = 135 (14-08-2025)

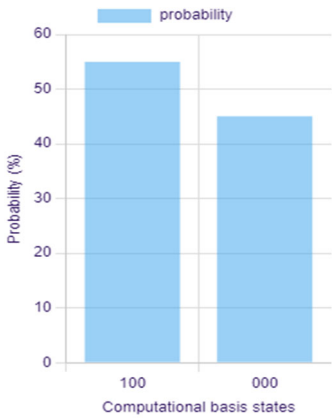

Temp = 124 Pre = 49
Hum = 129 (15-08-2025)

Fig. 5. cont.

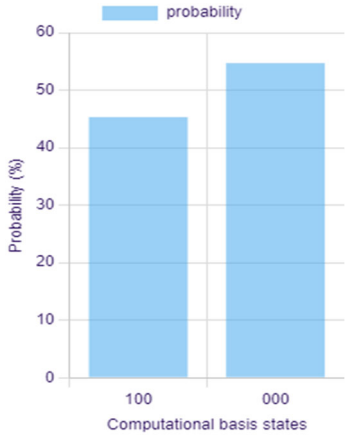

Temp = 125 Pre = 49
Hum = 136 (16-08-2025)

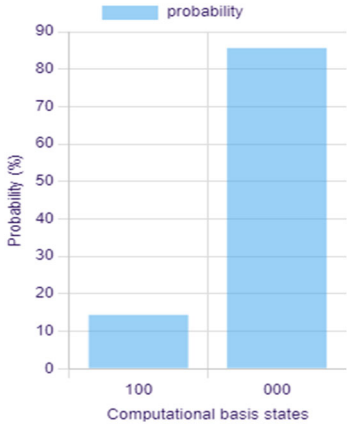

Temp = 123 Pre = 50
Hum = 144 (17-08-2025)

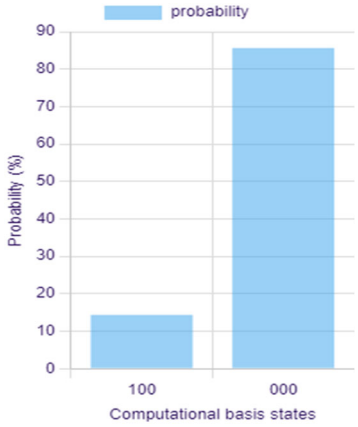

Temp = 122 Pre = 50
Hum = 137 (18-08-2025)

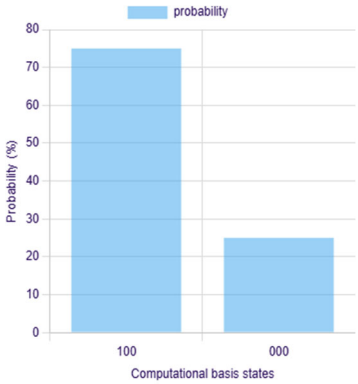

Temp = 122 Pre = 51
Hum = 122 (19-08-2025)

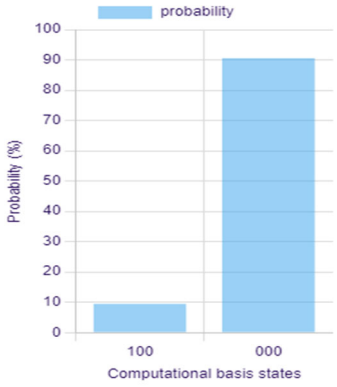

Temp = 126 Pre = 50
Hum = 122 (20-08-2025)

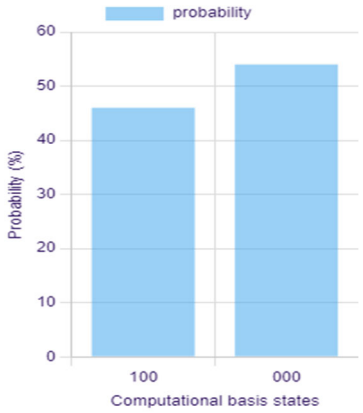

Temp = 127 Pre = 49
Hum = 129 (21-08-2025)

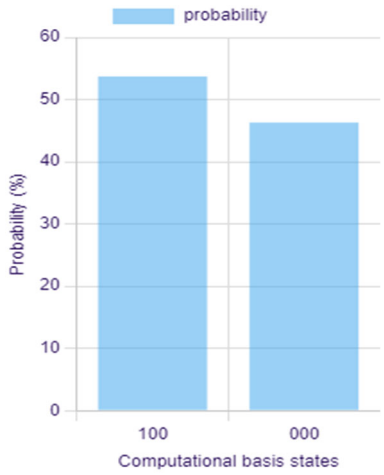

Temp = 126 Pre = 50
Hum = 143 (22-08-2025)

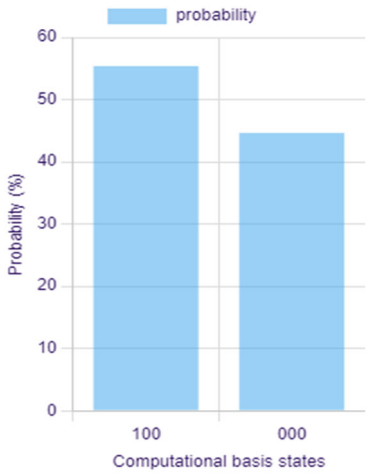

Temp = 122 Pre = 49
Hum = 149 (23-08-2025)

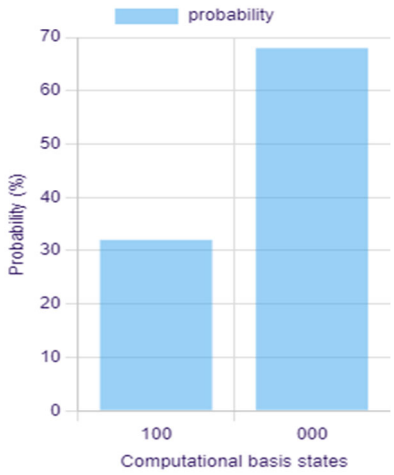

Temp = 125 Pre = 51
Hum = 134 (24-08-2025)

Fig. 5. cont.

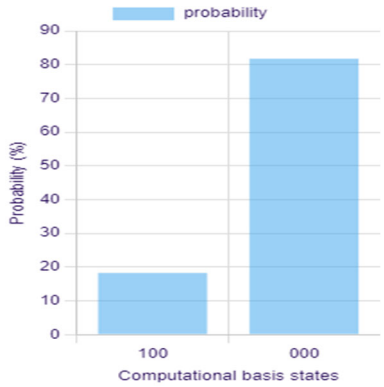

Temp = 123 Pre = 51
Hum = 132 (25-08-2025)

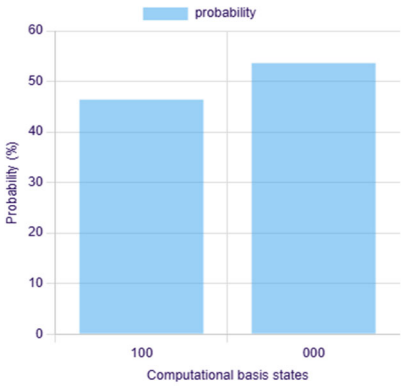

Temp = 124 Pre = 49
Hum = 134 (26-08-2025)

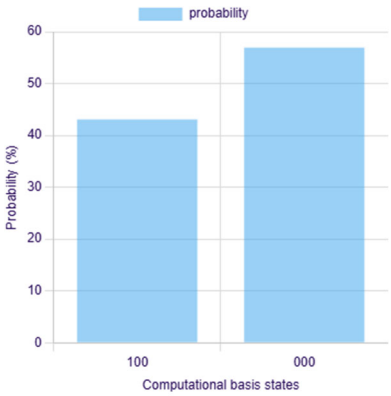

Temp = 124 Pre = 49
Hum = 133 (27-08-2025)

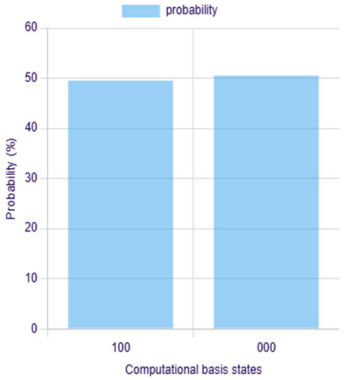

Temp = 125 Pre = 49
Hum = 130 (28-08-2025)

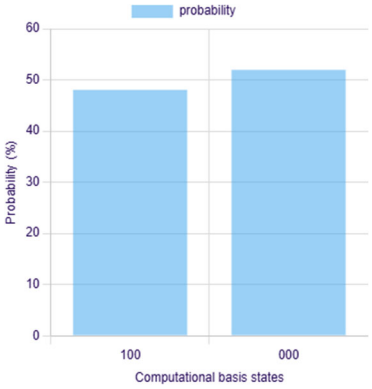

Temp = 127 Pre = 48
Hum = 131 (29-08-2025)

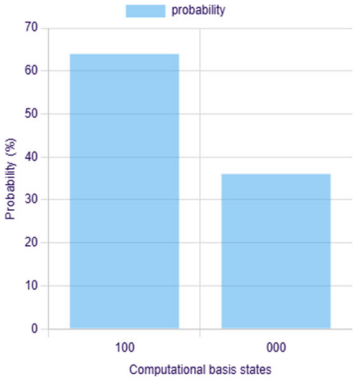

Temp = 126 Pre = 48
Hum = 130 (30-08-2025)

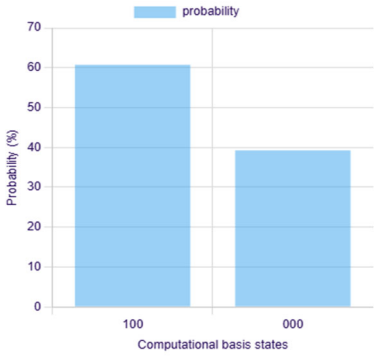

Temp = 126 Pre = 47
Hum = 159 (31-08-2025)

Fig. 5. cont.

The predictive accuracy bias arises from the quantum predictive model's tendency to favor the majority class in the training data. Because rainfall events account for the largest number of occurrences during the time period being observed, it is much more likely that the probabilities will collapse toward the rainfall state, resulting in high rainfall prediction accuracy and low no-rainfall prediction accuracy. This phenomenon is purely a function of the distribution of classes and is not indicative of any limitation in the quantum-encoding mechanism used to generate predictions.

The experimental and evaluation results for the SpinQ Gemini Lab Pro are shown in Figures 6 and 7. The implemented quantum circuit for rainfall prediction demonstrates high coherence and robust performance. The experimental results show a quantum state purity of 100%**,** confirming that the system maintained a fully pure quantum state throughout the computation, minimizing decoherence and external noise effects. The

experimental fidelity of 82.62% indicates that the realized quantum state closely matches the theoretically predicted one, validating the circuit's reliability for quantum-based data processing. The density matrix values (|0⟩ = 0.04, |1⟩ = 0.96) and Bloch sphere coordinates (0.04, -0.40, -0.92) reveal that the qubit state is strongly aligned toward the |1⟩ state, corresponding to a high-probability rainfall prediction scenario. The system exhibited minimal frequency error (-6.71 Hz) and stable control parameters, confirming precise pulse execution across the three-qubit configuration. Overall, the results validate the feasibility of using quantum gates such as R_x, R_y, R_z, and CNOT to model nonlinear environmental dependencies, providing a novel approach to rainfall prediction using quantum computing frameworks. A quantum simulator was used to validate the circuit's operation by running simulations on it. We need to build this circuit on a quantum computer to test how it behaves with actual devices and in the presence of real-world sources of interference (e.g., background noise and other phenomena), while also allowing for different levels of fidelity.

Fig. 6. Experimental result of SpinQ for rainfall prediction

Fig. 7. Evaluation result of SpinQ for rainfall prediction

Table 4 compares the proposed Hybrid Quantum Machine Learning model, developed using the SpinQ Gemini Lab Pro platform, with numerous published classical and ensemble rainfall prediction models from the literature. The model achieved an accuracy of 87.99%, indicating it performs competitively with traditional methods. In a study using historical meteorological data (2009–2023) from urban flooding areas in India, Sunil Khatri and Rajani P.K. (2025) reported accuracies for their models as follows: 80.11% for Long Short-Term Memory (LSTM), 70.96% for Support Vector Machine (SVM), 69.89% for Polynomial Regression, 68.14% for Random Forest, and 65.65% for eXtreme Gradient Boosting (XGBoost). Additionally, when utilizing long-term daily weather data collected over 111 years (1913–2023) by the Agro Climate Research Centre at Tamil Nadu Agricultural University in Coimbatore (semi-arid region), the researchers reported that the Multilayer Perceptron Neural Network (MLP) produced an accuracy of 85.55% and the Ran-

dom Forest Regressor produced an accuracy of 86.50%. On top of those datasets from Indian cities, Hussain and Aslam (2024) found that an Ensemble Classifier applied to the Bangladesh Weather Dataset (2013–2022) achieved an accuracy of 83%, while Ojugo and Ejeh (2023) found that a fused hybrid deep learning ensemble model applied to the weather data from Lagos, Nigeria (1999–2019) achieved an accuracy of 74%.

Table 4. Comparative table of rainfall prediction

Method / Model	Dataset / Region	Rainfall Accuracy (%)	Reference
SpinQ Gemini Lab Pro (Hybrid QML)	Experimental / Local Meteorological Data	87.99	This work
(Long Short-Term Memory) LSTM	Historical meteorological data (2009–2023), Indian regions – urban flood-prone areas (e.g., Mumbai)	80.11	(Sunil Khatri, Rajani P.K., 2025)
XGBoost	Same dataset (2009–2023, India)	65.65	(Sunil Khatri, Rajani P.K., 2025)
Random Forest	Same dataset (2009–2023, India)	68.14	(Sunil Khatri, Rajani P.K., 2025)
Polynomial Regression	Same dataset (2009–2023, India)	69.89	(Sunil Khatri, Rajani P.K., 2025)
Support Vector Machine (SVM)	Same dataset (2009–2023, India)	70.96	(Sunil Khatri, Rajani P.K., 2025)
Multilayer Perceptron Neural Network (MPNN)	Historical daily weather data (1913–2023), Agro Climate Research Centre, Tamil Nadu Agricultural University, Coimbatore (Semi-arid region)	85.55	(Sunil Khatri, Rajani P.K., 2025)
Random Forest Regressor (RFR)	Same dataset (1913–2023, Coimbatore region)	86.50	(Sunil Khatri, Rajani P.K., 2025)
Ensemble Classifier	Bangladesh Weather Dataset (from 2013 to 2022)	83	(Hussain, A., Aslam, 2024)
Fused hybrid deep learning ensemble	Metrological Center in Lagos, Nigeria, for the period 1999–2019	74	(Ojugo, A. A., Ejeh, P. O, 2023)

Regardless of variations between studies regarding dataset features, climate regions, and time periods, the new hybrid QML model exhibited similar or superior levels of predictive accuracy as compared to other established machine learning (ML) and deep learning (DL) models, thus showing the possible advantage of utilizing quantum-enhanced representation of input data for making predictions about rainfall.

3. Conclusion

In this work, rainfall detection was predicted using a quantum circuit–based approach, where temperature, pressure, and humidity were encoded into quantum states through $R_y(\theta)$ rotations. The introduction of CNOT gates enabled entanglement, thereby capturing correlations among meteorological variables, while the inclusion of variational layers with parameterized $R_y(\phi)$ and $R_x(\phi)$ gates allowed the model to learn complex nonlinear relationships efficiently. Meteorological data from August 1 to August 31 were utilized to

validate the proposed methodology, and the outputs were analyzed to determine the likelihood of rain and no-rain events. Theoretically, the quantum rainfall model achieved a fidelity of 87.99%. In contrast, the experimental implementation on the SPINQ Gemini platform yielded a quantum state purity of 100% and a fidelity of 82.62%, with density matrix values ($|0\rangle = 0.04$, $|1\rangle = 0.96$) indicating a strong probability of rainfall. Overall, the proposed hybrid quantum-classical framework achieved rainfall prediction accuracy of 87.99% and no-rain accuracy of 12.01%, demonstrating the effectiveness of quantum computation in modelling nonlinear meteorological dependencies and highlighting its potential to advance next-generation weather forecasting models.

Author Contribution

Mariselvam A.K: Conceptualization, Methodology, Formal Analysis, Investigation, Writing – Original Draft, and Writing – Review & Editing.
Mohamed Nizar S: Conceptualization, Methodology, Investigation, Writing – Original Draft, Writing – Review & Editing.
S. Sasikumar: Formal Analysis, Writing – Original Draft, and Writing – Review & Editing.
Vieeralingaam G: Methodology, Investigation, and Writing – Review & Editing.

Conflict of Interest

The authors declare that they have no conflict of interest

Authors' Statement

The authors declare that the work presented in this manuscript is original and has not been published elsewhere, nor is it currently under consideration for publication by any other journal. All authors have contributed significantly to the research and the preparation of the manuscript. They have read and approved the final version and agree to be accountable for all aspects of the work in ensuring that questions related to the accuracy or integrity of any part of the work are appropriately investigated and resolved.

Acknowledgment

The authors sincerely acknowledge the funding support and resources provided by *Rajalakshmi Institute of Technology, Chennai, India*.

References

Bauer, P., Thorpe, A., & Brunet, G. (2015). The quiet revolution of numerical weather prediction. *Nature*, *525*(7567), 47–55. https://www.nature.com/articles/nature14956

Benedetti, M., Lloyd, E., Sack, S., & Fiorentini, M. (2019). Parameterized quantum circuits as machine learning models. *Quantum Science and Technology*, *4*(4), 043001. https://iopscience.iop.org/article/10.1088/2058-9565/ab4eb5/pdf

Biamonte, J., Wittek, P., Pancotti, N., Rebentrost, P., Wiebe, N., & Lloyd, S. (2017). Quantum machine learning. *Nature*, *549*(7671), 195–202. https://www.nature.com/articles/nature23474

Farhi, E., & Neven, H. (2018). Classification with quantum neural networks on near-term processors. arXiv preprint, arXiv:1802.06002. https://arxiv.org/abs/1802.06002

Havlíček, V., Córcoles, A.D., Temme, K., Harrow, A.W., Kandala, A., Chow, J.M., & Gambetta, J.M. (2019). Supervised learning with quantum-enhanced feature spaces. *Nature*, *567*(7747), 209–212. https://arxiv.org/pdf/1804.11326

Hussain, A., Aslam, A., Tripura, S., Dhanawat, V., & Shinde, V. (2024). *Weather forecasting using machine learning techniques: Rainfall and temperature analysis*. https://doi.org/10.20944/preprints202402.1566.v2

Jayawardene, H., Sonnadara, D., & Jayewardene, D. (2005). Trends of rainfall in Sri Lanka over the last century. *Sri Lankan Journal of Physics*, *6*, 7–17. https://sljp.sljol.info/articles/197/files/submission/proof/197-1-796-1-10-20081107.pdf

Kandasamy, O., Maragatham, N., Somasundaram, E., Ravikumar, R., Kannan, B., & Pradipa, C. (2025). Rainfall prediction using artificial neural networks and machine learning algorithms over the Coimbatore region. *Journal of Water and Climate Change*, *16*(3), 946–959. https://iwaponline.com/jwcc/article/16/3/946/107335

Khatri, S. & K.P., R.P. (2025). Advanced weather forecasting with machine learning: Leveraging meteorological data for improved predictions. *Communications on Applied Nonlinear Analysis*, *32*(5s), ISSN: 1074-133X.

Nielsen, M.A., & Chuang, I.L. (2010). *Quantum Computation and Quantum Information*. Cambridge University Press, Cambridge. https://profmcruz.wordpress.com/wp-content/uploads/2017/08/quantum-computation-and-quantum-information-nielsen-chuang.pdf

Ojugo, A.A., Ejeh, P.O., Odiakaose, C.C., Eboka, A.O., & Emordi, F.U. (2026). Predicting rainfall runoff in Southern Nigeria using a fused hybrid deep learning ensemble. *International Journal of Informatics and Communication Technology (IJ-ICT)*, *13*(1), 108-115. file:///C:/Users/Admin/Downloads/20677-39459-1-PB%20(1).pdf

Olatayo, T.O., & Taiwo, A.I. (2014). Statistical modelling and prediction of rainfall time series data. *Global Journal of Computer Science and Technology*, *14*, 1–9.

Palmer, T.N., Doblas-Reyes, F.J., Hagedorn, R. & Weisheimer, A. (2005). Representing model uncertainty in weather and climate prediction. *Annual Review of Earth and Planetary Sciences*, *33*, 163–193. https://www.annualreviews.org/doi/10.1146/annurev.earth.33.092203.122552

Pour, S.H., Harun, S.B. & Shahid, S. (2014). Genetic programming for the downscaling of extreme rainfall events on the east coast of Peninsular Malaysia. *Atmosphere*, *5*, 914–936. https://www.mdpi.com/2073-4433/5/4/914

Pratomo, A.H., Santosa, B., Tahalea, S.P., Paripurno, E.T., Prasetyo, J.D., Jayadianti, H., & Pitayandanu, M.F. (2022). Rainfall prediction using artificial neural networks with historical weather data as supporting parameters. *Jurnal Informatika*, *16*(2), 63–73. https://ejournal.akademitelkom.ac.id/j_ict/index.php/j_ict/article/view/253

Rasp, S., & Lerch, S. (2018). Neural networks for postprocessing ensemble weather forecasts. *Monthly Weather Review*, *146*(11), 3885–3900. https://journals.ametsoc.org/view/journals/mwre/146/11/mwr-d-18-0187.1.xml

Rotunno, R., & Snyder, C. (2008). A generalization of Lorenz's model for the predictability of flows with many scales of motion. *Journal of the Atmospheric Sciences*, *65*, 1063–1076.

Shahid, S. (2011). Trends in extreme rainfall events of Bangladesh. *Theoretical and Applied Climatology*, *104*, 489–499. https://link.springer.com/article/10.1007/s00704-010-0363-y

Slingo, J., & Palmer, T. (2011). Uncertainty in weather and climate prediction. *Philosophical Transactions of the Royal Society A*, *369*, 4751–4767. https://royalsocietypublishing.org/doi/10.1098/rsta.2011.0161

Smadi, M.M., & Zghoul, A. (2006). A sudden change in rainfall characteristics in Amman, Jordan during the mid-1950s. *American Journal of Environmental Sciences*, *2*, 84–91. https://www.cabidigitallibrary.org/doi/full/10.5555/20073213158

Su, B.D., Jiang, T., & Jin, W.B. (2006). Recent trends in observed temperature and precipitation extremes in the Yangtze River basin, China. *Theoretical and Applied Climatology*, *83*, 139–151. https://link.springer.com/article/10.1007/s00704-005-0139-y

UCAR Center for Science Education, 2021. Climate Change: Regional Impacts. UCAR, Boulder, CO, USA. https://scied.ucar.edu/learning-zone/climate-change-impacts/regional

Wilson, L., Manton, M.J. & Siems, S.T. (2013). Relationship between rainfall and weather regimes in south-eastern Queensland, Australia. *International Journal of Climatology*, *33*, 979–991. https://rmets.onlinelibrary.wiley.com/doi/10.1002/joc.3484